Identification of Red Pigments Produced by Cheese-Ripening Bacterial Strains of *Glutamicibacter arilaitensis* Using HPLC

Nuthathai Sutthiwong [1,*], Piyada Sukdee [1], Supaporn Lekhavat [1] and Laurent Dufossé [2,*]

1   Expert Centre of Innovative Health Food (InnoFood), Thailand Institute of Scientific and Technological Research, Technopolis 35 Mu 3, Klong Ha, Klong Luang, Pathum Thani 12120, Thailand; piyada@tistr.or.th (P.S.); supaporn_pis@tistr.or.th (S.L.)

2   Chimie et Biotechnologie des Produits Naturels (CHEMBIOPRO), ESIROI Département Agroalimentaire, Université de La Réunion, Parc Technologique, 2 rue Joseph Wetzell, F-97490 Sainte-Clotilde, Ile de La Réunion, France

*   Correspondence: nuthathai@tistr.or.th (N.S.); laurent.dufosse@univ-reunion.fr (L.D.); Tel.: +66-25779130 (N.S.); +262-262217544 (L.D.)

Abstract: *Glutamicibacter arilaitensis* is one of the predominant bacterial species involved in the coloration of cheese rinds, especially smear-ripened cheeses. Besides well-known yellow-pigmented carotenoids, this species exhibits an ability to produce red pigments, as the occurrence of pink/red formation was previously found when co-cultured with a fungal strain. In this work, the red pigments synthesized by *G. arilaitensis* strains grown on cheese-based (curd) solid medium deacidified using *Debaryomyces hansenii* were identified. The analyses using HPLC equipped with both fluorescence and diode array detectors were performed to characterize the pigments extracted from a dry matter of the medium inoculated with either *G. arilaitensis* Re117, Po102, or Stp101. Based on the UV–vis absorption spectra, the elution order, and fluorescent property, compared to those of the porphyrin standards, eight metal-free porphyrins, including UPI, UPIII, 7PI, 6PI, 5PI, CPI, CPIII, and MPIX, were indicated as components of the red pigments produced by these *G. arilaitensis* strains. However, following the chromatographic profiles, the degree of porphyrins formed by each strain was apparently different. Regardless of precise quantitative measurement, the type strains Re117 and Po102 manifested a potential to produce a high amount of CPIII, whereas MPIX was formed by the strains Po102 and Stp101, but exceptionally high by the strain Stp101. The variation in both yield and form of the red pigments synthesized by the cheese-related bacterial *G. arilaitensis* has not previously been reported; therefore, our results provide the first information on these aspects.

Keywords: *Glutamicibacter arilaitensis*; red pigment; cheese rind

1. Introduction

Smear-ripened cheeses are among dairy products that are widely consumed, particularly in Europe. The colors of these cheese rinds, which are the result of pigment synthesis by complex surface microflora, play an important role in a consumer's purchasing decision [1,2]. Unconventional color characteristics of cheeses can contribute to economic losses for producers because they possibly link to consumers' misunderstanding of the quality of cheeses [3].

Pink pigmentation has commonly been identified as a defect in a broad range of cheeses. Different formations of this discoloration depending on cheese types are found, for example, occurring at the surface of the cheese block, diffusing within the cheese block, and arising as a ring uniform under the cheese rind [4–6]. Factors affecting pink discoloration are reportedly related to the change of physicochemical and microbial properties [7–9]. In terms of the microbial attribute, several studies have been detailed for a few decades that certain strains of starter cultures used for cheese production can synthesize

red pigments; e.g., *Microbacterium gubbeenense*, *Thermus thermophilus*, *Lactobacillus* sp., and *Arthrobacter sp*. [10–14].

Arthrobacter arilaitensis (presently named *Glutamicibacter arilaitensis*—to be up to date, *G. arilaitensis* will be used throughout this article) is one of the important bacterial strains responsible for the pigmentation of cheese rinds due to its presence at different stages of the ripening process, principally at the middle and late stages [15,16]. Besides the yellow pigments, which were characterized as a group of C50 carotenoids consisting of eight forms, but mainly decaprenoxanthin, *G. arilaitensis* has recently been reported to synthesize red pigment(s) [17–19]. In our previous study [19], a strain of *G. arilaitensis*, Po102, evidently developed pink/red-brown color suffusing inside inoculated cheese-based (curd) solid media. After a tentative determination, the results showed that the pink pigments excreted by this strain were water-soluble and fluoresced under UV light. The UV–visible scanning of the extracts exhibited fine structure, with wavelengths of maximum absorption at 394, 497, 530, 567, and 620 nm. Corresponding to the recent information reported by Cleary et al. [20] and general characteristics of porphyrins (i.e., absorption spectra and fluorescence property), the pink/red-brown discovered would be pigments in the porphyrin series.

During recent decades, high-performance liquid chromatography (HPLC) has commonly been used as a technique for separating and identifying complex mixtures of molecules in food analysis because of such advantages as speed, high resolution, and sensitivity [21,22]. Several works on the identification of pigments produced by microorganisms used in cheese production were achieved by using HPLC [23–25]. The current work, therefore, applied this technique in order to characterize the pink/red-brown pigments produced by *G. arilaitensis* strains grown on cheese-based (curd) medium deacidified using *D. hansenii*.

2. Materials and Methods

2.1. Strains and Cultures

2.1.1. Bacterial and Yeast Strains

Three bacterial *Glutamicibacter arilaitensis* strains were selected for investigating their red-pigmented products in this work. The choice of 2 strains, namely *G. arilaitensis* Po102 and Stp101, was due to our previous works on their yellow pigmentation and combined effects of pH, NaCl, and deacidifying yeasts, in which red-brown pigmentation was incidentally found, while *G. arilaitensis* Re117 is the type strain of the species whose genome sequence was already revealed (nota bene: the type strain is also known under the following collection numbers: DSM 16,368/CIP 108,037/JCM 13566).

The strain, *Glutamicibacter arilaitensis* Po102, was isolated from cheeses in our laboratory, while the others, including the type strain Re117 and Stp101, and a deacidifying yeast *Debaryomyces hansenii* 304 were kindly provided by the Institut National de la Recherche Agronomique (INRA), Thiverval-Grignon, France. They were maintained during this study on a medium depending on their nutrient requirements (i.e., milk ingredient-based medium for bacteria or potato dextrose agar for yeasts, as described below), stored at 4 °C, and subcultured monthly.

2.1.2. Cultures

Potato dextrose broth (PDB; BD Biosciences, Le Pont de Claix, France) was used as a subculture medium for *D. hansenii* 304, while the milk ingredient-based medium was prepared and used for the *G. arilaitensis* strains. A milk ingredient-based liquid medium containing 5 g casamino acids (BD Biosciences, Le Pont de Claix, France), 1 g yeast extract (BD Biosciences, Erembodegem, Belgium), 5 g NaCl (Fisher Scientific, Illkirch-Graffenstaden, France), 20 g D-glucose (HiMedia, Nashik, India), and 1 g KH_2PO4 (HiMedia, Nashik, India) per liter of deionized water, was prepared. Before sterilizing at 121 °C for 15 min, the pH of the medium was adjusted to 7.0 ± 0.2 using 1 M NaOH (ACROS Organics, Geel, Belgium).

To prepare a microbial suspension, *D. hansenii* 304 was inoculated into a 250 mL Erlenmeyer flask containing 50 mL PDB, whereas the milk ingredient-based liquid medium was used instead of PDB for the *G. arilaitensis* strains. These flasks were incubated at 25 °C with agitation at 150 rpm for 2 days. After the cultivation period, the cells were harvested by centrifugation at $6000\times g$ for 10 min and resuspended in peptone saline diluent (1 g casein peptone (Sigma-Aldrich, Darmstadt, Germany) and 8.5 g NaCl (HiMedia, Nashik, India)) adjusted to 7.0 ± 0.2 at 25 °C. A suspension containing 10^7 cells mL^{-1} was prepared to be used in the next step.

A cheese-based (curd) solid medium was used to cultivate the strains of *G. arilaitensis* for the production of red pigments. The procedure for preparing the experimental medium employed in this study was adapted according to our previous work [19]. Whole milk was used to form a cheese curd via rennet coagulation. Before preparing the cheese-based medium, the frozen cheese curd, which was kept at −80 °C to prevent an enzymatic reaction, was thawed at 4 °C for roughly 24 h. The defrosted cheese curd was mixed with distilled water (60% *w/v*); then the mixture was homogenized using a blender and placed in a water bath (95 °C) for 30 min. Seventeen grams of agar and 2% NaCl (*w/v*) were added into the cheese slurry, and its pH was adjusted to 7.5, with 1 M NaOH. The final mixture was blended again until the texture was homogeneous, then pasteurized by heating at 80 °C for 10 min. After cooling down to 45–50 °C, the pour plate technique was used to prepare the cheese-based (curd) solid medium contained in Petri dishes, which were left to solidify for 2 h before inoculation with cheese-ripening strains.

2.2. Sample Preparation

2.2.1. Pigment Production

One mL of 10^7 cell suspension of *D. hansenii* 304 was spread over the surface of the cheese-based (curd) solid medium. All Petri dishes were then incubated at 25 °C for 7 days. Afterward, 1 mL of a 10^7 cell suspension of either *G. arilaitensis* strain was inoculated onto the surface of the medium, which thereafter was cultivated at 25 °C under the light.

2.2.2. Pigment Extraction and Purification

Selected Petri dishes containing media of either *G. arilaitensis* strain, which displayed pink/red-brown color, were lyophilized. A dry matter of each strain was totaled, and then individually extracted with ethyl acetate (VETEC, Bangalore, India) and acetic acid (Merck, Darmstadt, Germany) in a ratio of 3:1 (*v/v*) using an ultrasonic bath for 10 min. A suspension was centrifuged ($6000\times g$, 15 min), and later transferred the supernatant to a fresh tube. An aliquot of deionized water was added to the supernatant, then mixed vigorously and centrifuged at $7000\times g$ for 5 min. The aqueous top layer was removed and discarded, whereas the organic one containing pink/red pigments was collected. The extraction was repeated until the supernatant and residual pellet were colorless.

All supernatants were mixed and evaporated under a vacuum. The concentrated sample was loaded onto a C18 Sep-Pak cartridge (Waters, Wexford, Ireland), which was conditioned and equilibrated with 4 mL acetonitrile (Merck, Darmstadt, Germany), 4 mL deionized water, and 4 mL formic acid (Sigma-Aldrich, Darmstadt, Germany) solution (0.1% *v/v*). The pink/red-brown pigments were washed sequentially with 4 mL deionized water, 4 mL formic acid solution, 4 mL acetonitrile/deionized water (5:95, *v/v*), and 4 mL acetonitrile.

The pigmented eluate was evaporated to dryness under a vacuum. Then, 1 mL of 3 M HCl (Merck, Darmstadt, Germany) was added to dissolve the residue, followed by filtering through a 0.45 μm PTFE syringe filter (Sartorius, Goettingen, Germany).

2.3. High-Performance Liquid Chromatography Analysis

2.3.1. Apparatus

The HPLC analysis was performed using a Dionex Ultimate 3000 liquid chromatograph (Thermo Fisher Scientific, Courtaboeuf, France) equipped with the following parts:

FLD-3400 RS fluorescence detector, DAD-3000 diode array detector, LPG-3400 SD pump, WPS-3000 TSL autosampler, and TCC-3000 SD column component. Monitoring, data recording, and processing were driven with the CHROMELEON 7 software (Dionex).

2.3.2. Chromatographic Condition

The separation was conducted on a Hypersil BDS C18 column (250 × 4.6 mm, 5 μm, Thermo Scientific) with a mobile phase flow rate of 0.4 mL/min. The temperatures of autosampler and column were set at 5 °C and 35 °C, respectively. The fluorescence detector was adjusted at excitation of 400 nm and emission of 620 nm. The multilinear gradient applied was slightly modified from a previous study by Benton et al. [26] A mobile phase system consisted of two components, including 10% (*v/v*) acetonitrile in 1 M ammonium acetate–acetic acid buffer, pH 5.17 (solvent A), and 10% (*v/v*) acetonitrile in methanol (solvent B). The elution program started with 0% B, then increased linearly to 30% B within 15 min, followed by another linear increase to 90% B from 15 to 30 min. Mobile phase B was held at 90% until the end of the elution program (55 min).

A CMK-1A chromatographic marker, containing a Type I series of 8-carboxyl porphyrin (uroporphyrin), 7-carboxyl porphyrin (heptaporphyrin), 6-carboxyl porphyrin (hexaporphyrin), 5-carboxyl porphyrin (pentaporphyrin), and 4-carboxyl porphyrin (coproporphyrin), and mesoporphyrin IX, was purchased from Frontier Scientific (Logan, UT, USA). Two individual porphyrin standards; namely, uroporphyrin III tetramethyl ester and coproporphyrin III octamethyl ester, were obtained from Sigma-Aldrich (St Louis, MO, USA).

HPLC-grade chemicals and reagents were used thoroughly for the analysis as components of mobile phases. Ammonium acetate, acetonitrile, methanol, and acetic acid were acquired from Merck (Darmstadt, Germany). Deionized water at 18 Ω was produced by a Smart2Pure 6 UV/UF ultrapure water system from Thermo Scientific (Langenselbold, Germany).

3. Results

3.1. HPLC Separation of Porphyrins

The reversed-phase HPLC paired with fluorescence detection allowed the simultaneous separation of a mixture of porphyrin standards used in this study (Figure 1). The chromatogram demonstrated the respective porphyrin isomers I and III in the series within 55 min. Depending upon the decreasing number of carboxylic acid groups attached to the basic porphine structure, the porphyrin isomers were sequentially eluted: uroporphyrin I (UPI), uroporphyrin III (UPIII), 7-carboxyl porphyrin (7PI), 6-carboxyl porphyrin (6PI), 5-carboxyl porphyrin (5PI), coproporphyrin I (CPI), coproporphyrin III (CPIII), and mesoporphyrin IX (MPIX). Although 2 peaks appeared during min 23–24, both were counted as 6PI. The separation of the 6PI into 2 peaks was feasibly affected by the difference in elution times between *cis* and *trans* isomers contained in the authentic 6PI [27]. The chemical structures of these isomers are shown in Figure 2.

The recorded UV–vis absorption spectra of each chromatographic peak of the porphyrin standard mixture (Figures S1–S9) were noted in terms of Soret band and Q bands (Table 1), according to electronic transitions from the ground state (S0) to the two lowest singlet excited states S1 and S2 (for a full explanation of the Soret band and Q bands, see Appendix A).

3.2. Identification of Red Pigments Produced by G. arilaitensis Strains

The *G. arilaitensis* cultured media contained in Petri dishes were selectively collected to get the maximum intensity of red pigments. After the extraction and purification, the extracts were analyzed using the described HPLC method. Three aspects, including fluorescent property, retention time, and UV–vis absorption spectra were recorded.

Besides their fluorescent property as displayed in Figure 3, pigments were identified based on their retention time and UV–vis spectra compared to those of authentic standards. Typical chromatograms of the extracts of each *G. arilaitensis* strain are shown in Figure 4.
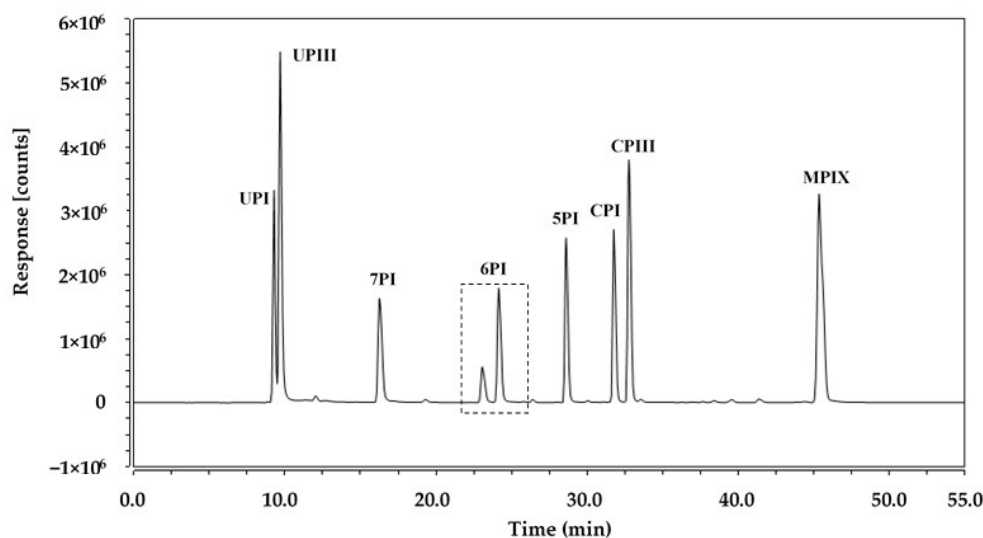
Figure 1. HPLC chromatographic profile of a porphyrin standard mixture. UPI: uroporphyrin I; UPIII: uroporphyrin III; 7PI: 7-carboxyl porphyrin; 6PI: 6-carboxyl porphyrin; 5PI: 5-carboxyl porphyrin; CPI: coproporphyrin I; CPIII: coproporphyrin III; MPIX: mesoporphyrin IX.
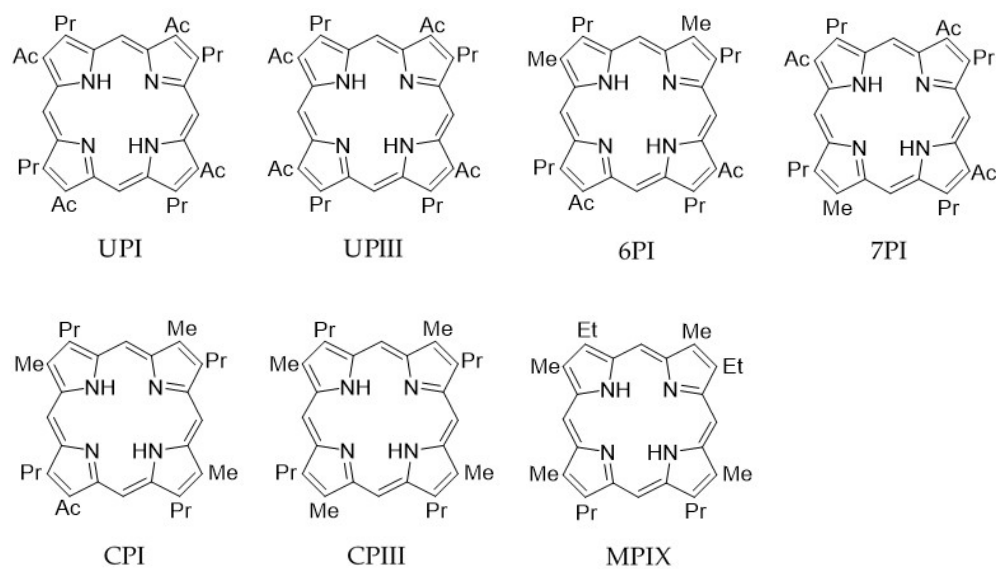

Figure 2. Structures of the porphyrin isomers. The β-positions of the four pyrrole rings are substituted with acetic acid (Ac), propionic acid (Pr), methyl (Me), and ethyl (Et). UPI: uroporphyrin I; UPIII: uroporphyrin III; 7PI: 7-carboxyl porphyrin; 6PI: 6-carboxyl porphyrin; 5PI: 5-carboxyl porphyrin; CPI: coproporphyrin I; CPIII: coproporphyrin III; MPIX: mesoporphyrin IX.

Table 1. Chromatographic and spectral properties of porphyrin standards.

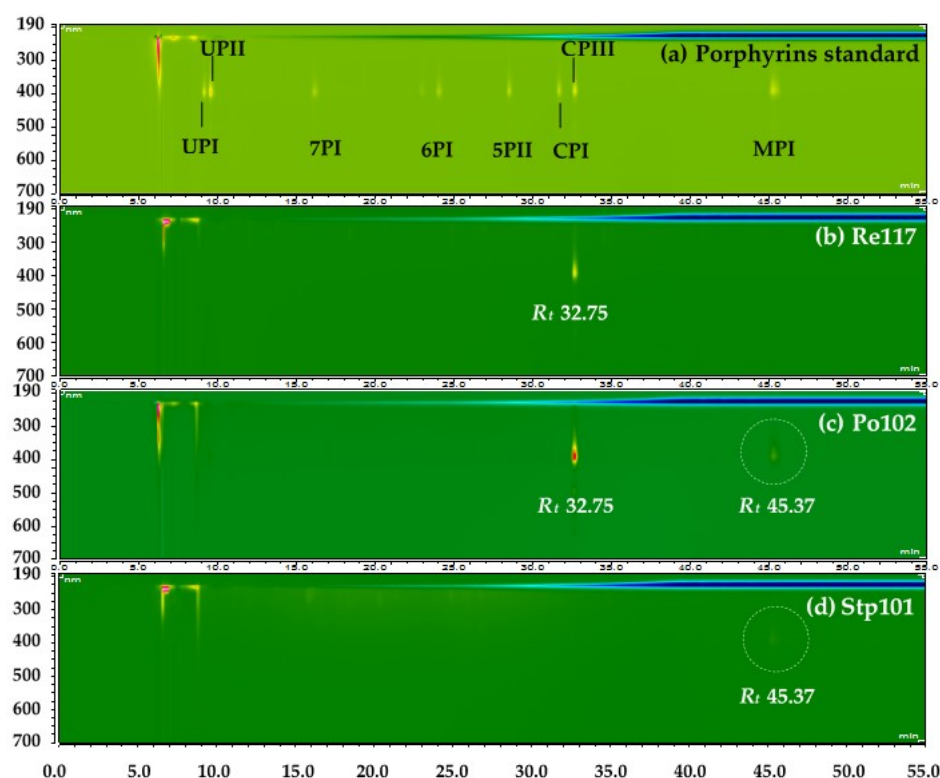| Porphyrins	R_t (min)	Soret Band λ (nm)	Q Band λ (nm)
UPI	9.28	398	501, 537, 563, 615
UPIII	9.68	398	501, 537, 563, 615
7PI	16.26	397	500, 536, 563, 615
6PI	23.06	396	500, 535, 564, 616
	24.14	396	500, 534, 564, 616
5PI	28.60	394	450, 533, 564, 617
CPI	31.77	393	497, 532, 564, 616
CPIII	32.76	393	497, 532, 564, 617
MPIX	43.35	392	496, 530, 565, 618

Figure 3. Fluorescent properties of porphyrin standard mixture (**a**) and red pigments extracted of *G. arilaitensis* strains, including (**b**) Re117, (**c**) Po102, and (**d**) Stp101.

According to the chromatographic profiles recorded at 400 nm excitation and 620 nm emission, compared with the retention time of the porphyrin standard mixture, eight porphyrin isomers were detected as components of red pigments produced by strains Re117, Po102, and Stp101. Among these components, only two isomers were displayed as major porphyrins following the figure of peaks presented on the chromatograms. The first peak was exhibited in a range of 32.75–32.79 min (Figure 4a–c), while the other was retained longer in the column and was eluted at min 45.37 (Figure 4b,c). The absorption spectra of these two principal peaks were composed of a Soret band and Q bands, as shown in Figures 5 and 6.

As shown in Figures 5 and 6, the spectral characteristics of the two major peaks perfectly matched those of CPIII and MPIX isomer standards; therefore, this could indicate that these *G. arilaitensis* strains predominantly produced CPIII and MPIX. However, there were differences in the production of porphyrins between these strains when we considered the pattern of chromatograms obtained from the HPLC analysis. CPIII was found to be the sole major porphyrin synthesized by the type strain *G. arilaitensis* Re117, whereas both CPIII and MPIX were exhibited in the extracts of *G. arilaitensis* Po102 and Stp101, but extremely high in *G. arilaitensis* Stp101. Other porphyrins, including UPI, UPIII, 7PI, 6PI, 5PI, and CPI, were present in trace amounts in the extracts of two strains, Po102 and Stp101, whereas the amount of MPIX was also low in the extract of the type strain Re117.
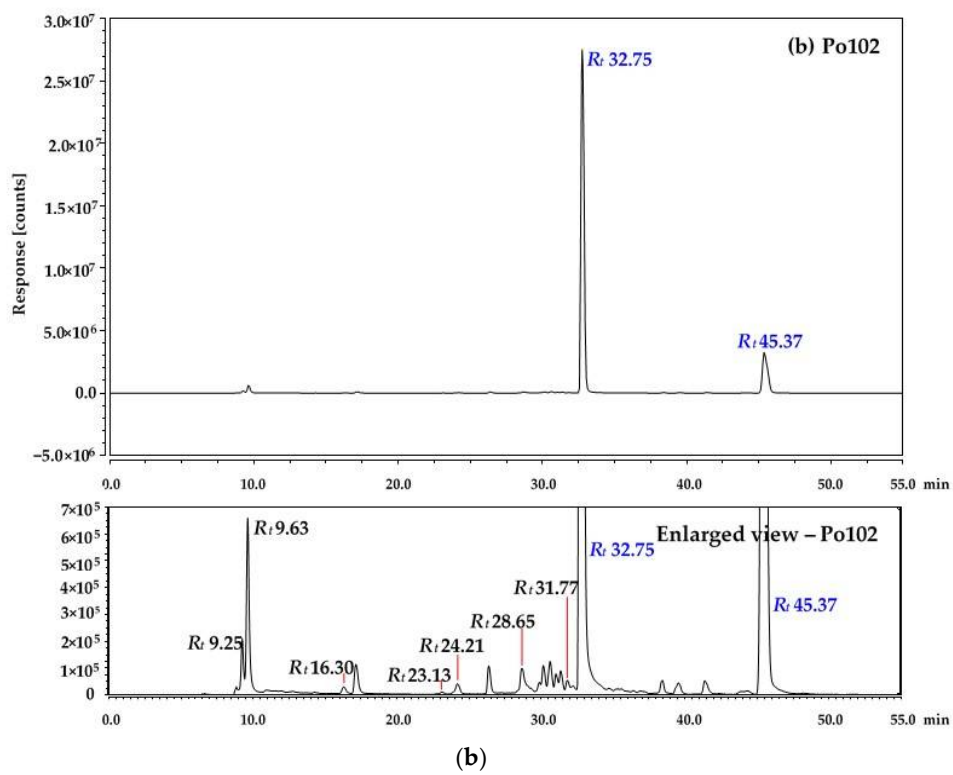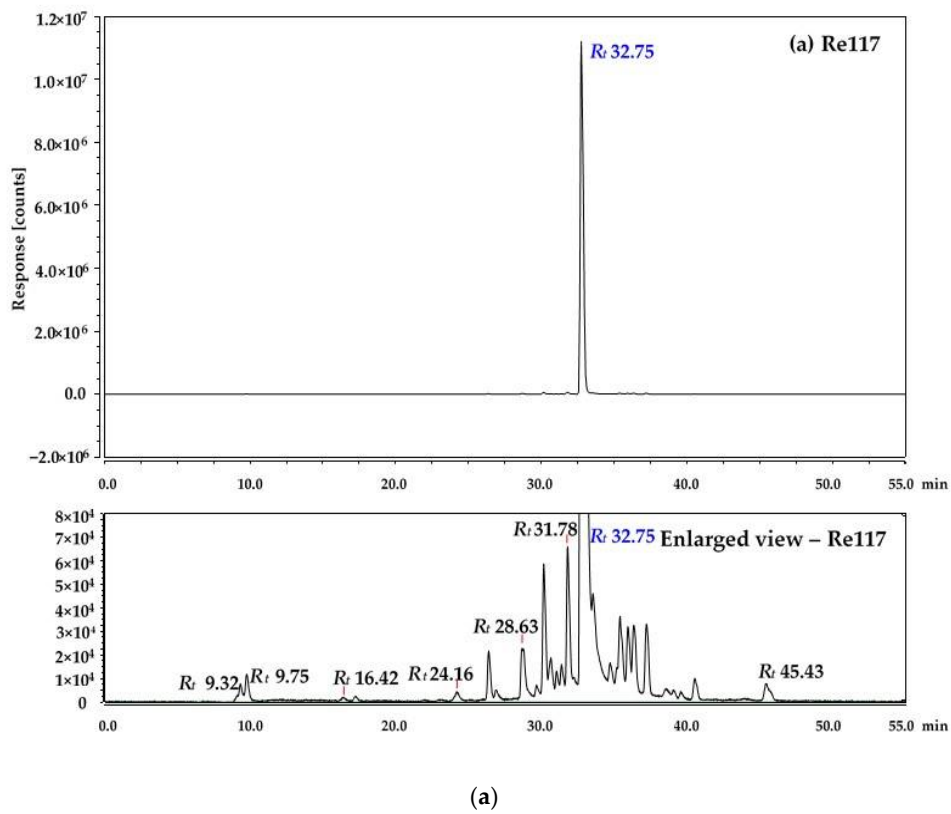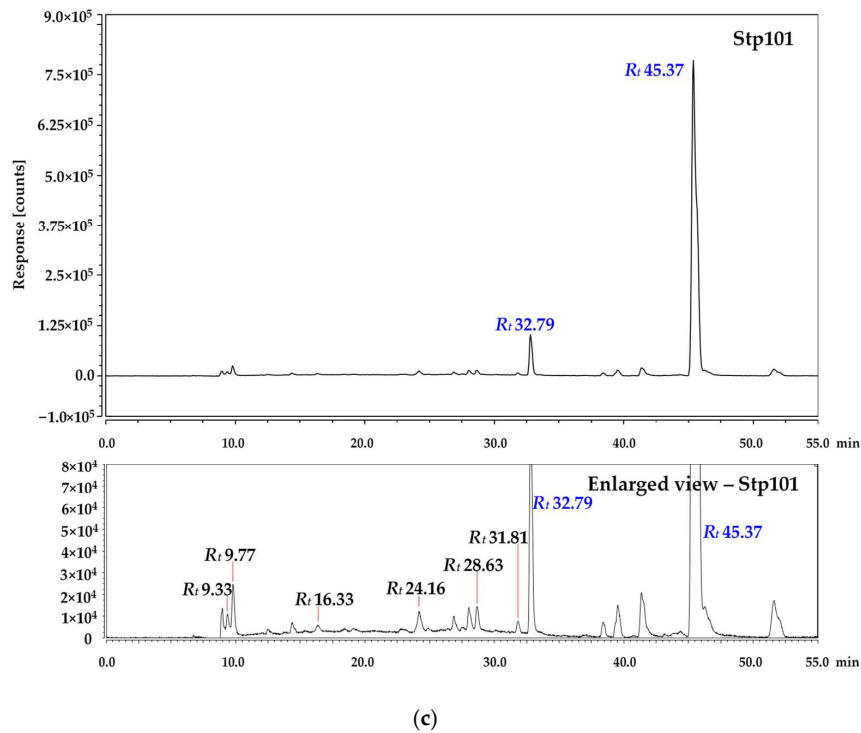
Figure 4. *Cont.*

Figure 4. HPLC chromatographic profiles of red pigments extracted of *G. arilaitensis* strains, including (**a**) Re117, (**b**) Po102, and (**c**) Stp101.
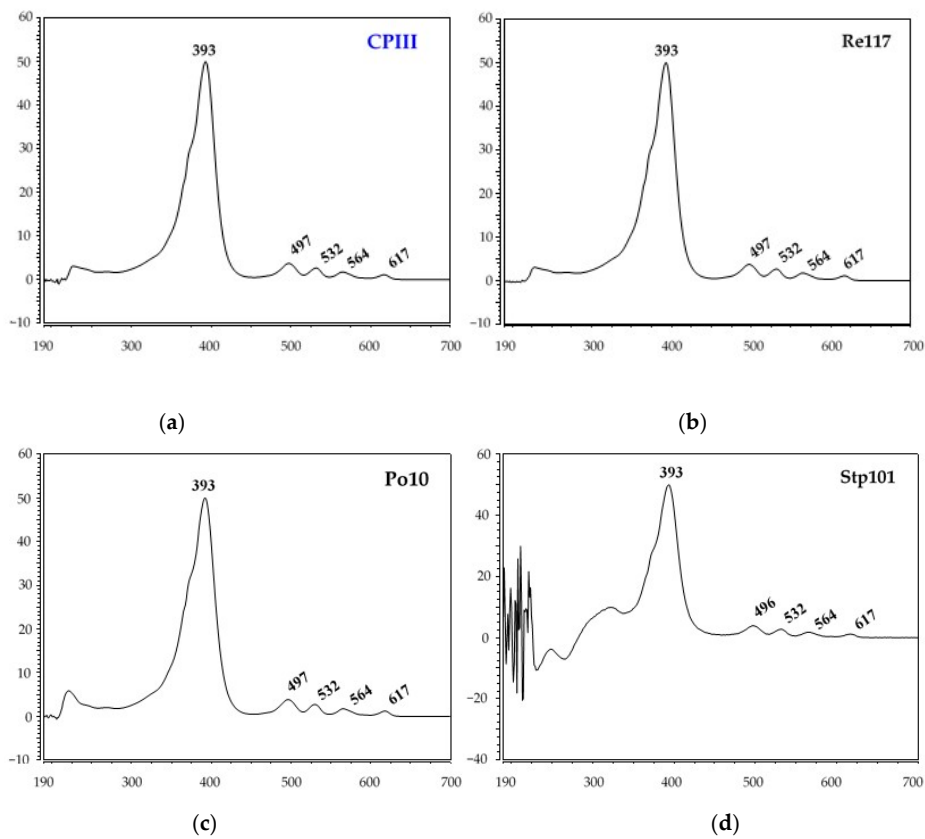

Figure 5. Comparison of absorption spectra of porphyrin standard, CPIII, and chromatographic peaks of the extracts exhibited at R_t about 32 min: (**a**) CPIII standard; (**b**) *G. arilaitensis* Re117 at R_t 32.75 min; (**c**) *G. arilaitensis* Po102 at R_t 32.75 min; (**d**) *G. arilaitensis* Stp101 at R_t 32.79 min.
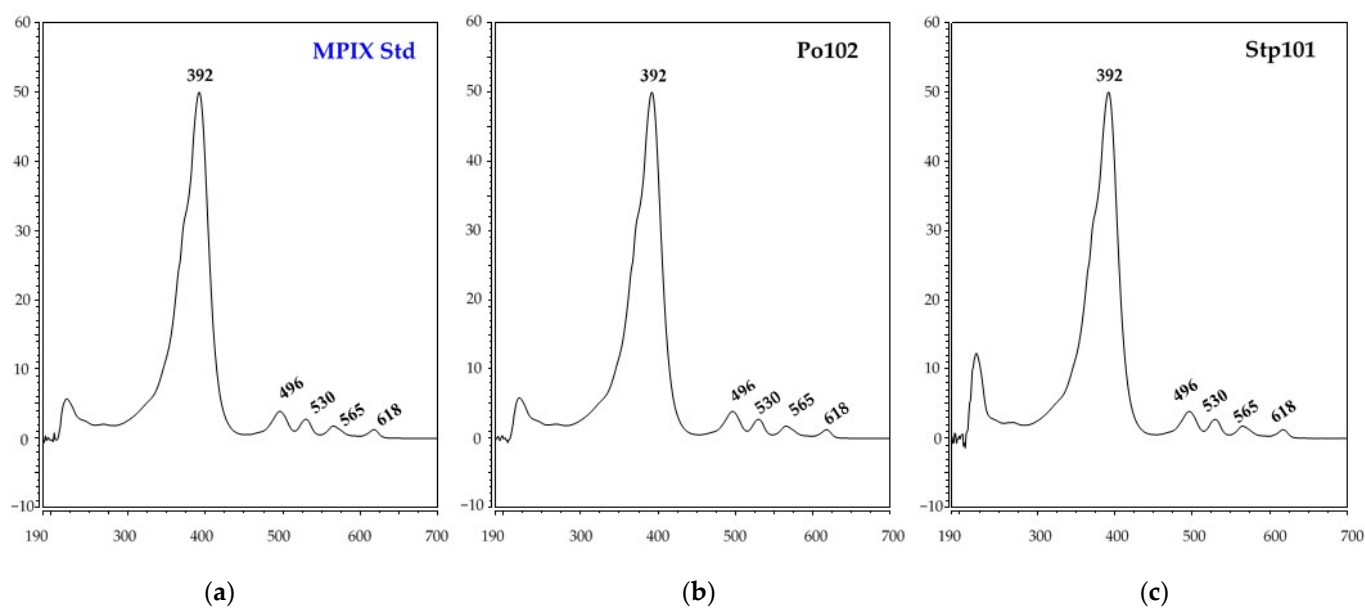
Figure 6. Comparison of absorption spectra of porphyrin standard, MPIX, and chromatographic peaks of the extracts exhibited at R_t about 45 min: (**a**) MPIX standard; (**b**) *G. arilaitensis* Po102 at R_t 45.37 min; (**c**) *G. arilaitensis* Stp101at R_t 45.37 min.

4. Discussion

The development of red/pink color in a variety of cheeses has long been reported as a defect that impacts the economic aspects of the cheese industry. In smear-ripened cheeses, pink/red-brown appearance—often called pink discoloration due to its undesirable characteristic relating to the quality of cheese—has been associated with certain microbial strains used as starter cultures for production. The mechanisms of color development of smear-ripening cheeses are still largely undefined because there are actions and correlations of a great number of microorganisms, both eukaryotes (primarily yeasts and molds) and prokaryotes (including pigmented and non-pigmented bacterial strains), during the cheese-making process [28].

For decades, only a few previous studies on the coloration of smear-ripening cheeses by *G. arilaitensis* were undertaken; thus, up to now, there are only two reports describing pink discoloration originated by this bacterial species. Recently, zinc CPIII was precisely characterized as a pink pigment produced by *G. arilaitensis* JB182, whereas in our earlier work, the red pigment extract of *G. arilaitensis* Po102 was assumed to be in a porphyrin cluster due to its characteristic UV–vis spectrum, which consists of two distinct regions in the near-ultraviolet and in the visible region, as well as its fluorescent property [19,20].

In this study, the pigments extracted from cultured media of *G. arilaitensis* strains, including the type strains Re117, Po102, and Stp101, originating from smear-ripened cheeses were qualitatively identified by an HPLC methodology. Via fluorescence detector and PDA, the red pigments were appropriately separated and able to be predicated. Based on the data of the absorption spectra and the elution order obtained from HPLC analysis, which matched against those of the standards, eight porphyrins were distinguished from the red-pigmented extracts of these three *G. arilaitensis* strains. As described in several experiments, it has been strongly suggested that changes in the conjugation pathway and symmetry of porphyrin can affect its UV–vis absorption spectra [29–31]. Mason et al. [32] reported that chelation of zinc by coproporphyrin excreted by *Actinomycetes* strains would extend retention time to slightly more polar elution and shift absorption spectra profile with a Soret band to a higher wavelength than the metal-free porphyrin. Lately, a similar phenomenon was found by Cleary et al. [20], who observed a pink pigment produced by a smeared-cheese bacterial *G. arilaitensis* strain. According to the results of LC-MS/MS analysis, the pigment was characterized to be zinc-bound coproporphyrin III, as its Soret

band shifted from 393 nm to 405 nm compared to the standard, which made it fit the description of zinc coproporphyrin III profiles. In addition, a study by Rostami et al. [33] reported a significant difference in the number of Q bands between free base porphyrins and metalloporphyrins, in that the metal-free porphyrins consisted of four peaks in the Q band region, while only two peaks were found from metalloporphyrins. Consequently, due to the fine compatibility with the standards and nonappearance of shifting in retention time and Soret band in their absorption-spectra profiles, the porphyrins by the *G. arilaitensis* strains studied (Re117, Po102, and Stp101) were affirmatively in metal-free forms; namely, UPI, UPIII, 7PI, 6PI, 5PI, CPI, CPIII, and MPIX. To the best of our knowledge, this is the first time that the simultaneous presence of eight metal-free porphyrins synthesized by the cheese-ripening bacterial strain *G. arilaitensis* was disclosed. Apart from these porphyrin isomers, it seemed that the three strains of *G. arilaitensis* also produced porphyrins in other forms, since there were several detectable peaks presented on the chromatograms. Among these peaks, some of them had enough intensity to display the fine absorption spectra (data not shown); for example, the peak of the extract of *G. arilaitensis* Stp101 that was eluted after MPIX (R_t 51.59 min), and peaks detected between R_t 32.75 and R_t 45.37 min of the injection of *G. arilaitensis* Po102 extract. Unfortunately, due to a limitation of available porphyrin standards, these peaks could not be identified in the current work.

Among microorganisms, several bacteria in the genus *Arthobacter*—of which certain strains were recently identified to belong to the genus *Glutamicibacter*, including *A. arilaitensis*—are reported for their abilities to synthesize pigments in porphyrin clusters [34]. Based on enzymes responsible for porphyrin biosynthesis, naturally occurring metal-free porphyrins exist only in type I and III isomer forms; nonetheless, CPIII and UPIII were shown to be the major porphyrins produced by *Arthrobacter* sp. [20,35–39]. In bacteria, these pigmented molecules are intermediate metabolites significantly involved in parts of energy-conserving electron-transport chains and co-factors of various enzymes; however, metal ions are required to chelate with the tetrapyrroles and bind to a specific protein for activating these functions [40,41]. Changes in physical and biochemical conditions usually induce an adaptation of bacterial energy metabolism, and often correspond to a huge alteration in the production of porphyrin [42,43].

Considering the accumulation of porphyrins in smear-ripened cheeses, microbial interactions are potential factors that affect these pink-pigmented compounds. For instance, CPIII formed in the presence of the *Penicillium* sp. when cultivated on blue cheese curd agar; thereby, it was described as part of the inhibitory effect of *G. arilaitensis* on *Penicillium* [20,44]. Two presumptions that could explain this phenomenon are the following: (1) the competition for metal ions between the bacterium and the fungus feasibly induces *G. arilaitensis* to produce CPIII, and (2) the fungus establishes a suitable environment enhancing the production of CPIII by *G. arilaitensis*. However, since all porphyrins identified from the Re117, Po102, and Stp101 strains in this study were in metal-free forms, the concept that the fungus provides a unique environment for the synthesis of porphyrins by *G. arilaitensis* seems to be a promising condition for this circumstance. This aligns with previous bacterium–fungus RNA-seq experiments in the interaction between bacterial and fungal strains isolated from cheese rind that expresses a significant increase in nutrient availability through proteolysis of cheese curd by fungi [20,45].

The pathway of tetrapyrrole biosynthesis in most bacteria proceeds by synthesizing a precursor metabolite, δ-aminolevulinic acid (ALA), from glutamate that binds glutamyl-tRNA by a glutamyl-tRNA-catalyzed reaction, then continues to synthesize intermediate metabolites, including porphobilinogen, uroporphyrinogen III, coproporphyrinogen III, protoporphyrinogen IX, protoporphyrin IX, and heme, respectively [46]. Metal-free porphyrins excreted by the *G. arilatensis* strains in this study were therefore not normal intermediate metabolites. Compared with hemes, metal-free porphyrins have not yet been shown to have a biological function, but the cell synthetic pathways have been interrupted. The pathways leading to functional tetrapyrroles; e.g., cytochromes, redox-active proteins containing a heme, have been blocked, thus engaging in the formation of one of the earlier

intermediates [47,48]. Besides, such interaction requires a compatible set of catalysts for each tetrapyrrole synthesis, so there will be a difference in the yield of each porphyrin depending on the type of enzyme synthesized by each bacterial strain [49,50]. This may describe the difference of the patterns of porphyrin formation by *G. arilaitensis* Re117, Po102, and Stp101, in that only CPIII was predominantly produced by the type strain Re117, while MPIX was found to be a major red pigment of strain Stp101, and ranged in the second of which by the strain Po102. The occurrence of MPIX was doubtful, since this molecule is not an intermediate in the biosynthesis of heme. It probably is related to the conversion of protoporphyrin IX (PPIX) into the more stable forms. In a study by Brazier [51], it was explained that PPIX is a labile structure with two vinyl side chains that incline to bacterial degradation; therefore, PPIX will be denatured and turn into MPIX.

Besides the carotenoids previously characterized and porphyrins identified in this study, interestingly, it seemed that the *G. arilaitensis* strains produced other fluorescent pigments. Corresponding to Figure 2, a small number of bands were found to express their fluorescent properties in a range of wavelengths between 200–400 nm at the beginning of the HPLC running program. Riboflavin could hypothetically be among these pigments due to its fluorescent property and the wavelength at which absorption occurs, and following several reports that found the ability of bacteria in the genus *Arthrobacter* to produce this vitamin [34,52].

5. Conclusions

Using the occurrence of pink discoloration during our previous study of the effect of certain factors on the coloration of *G. arilaitensis* strain isolated from smear-ripening cheese, this work aimed to identify the pink/red-brown pigments produced by this bacterial species. The pigments extracted from a dry matter of the cheese-based (curd) solid medium cultured with either *G. arilaitensis* Re117, Po102, or Stp101 were characterized using HPLC equipped with fluorescence and diode array detectors. The pigmented extracts were well separated by the analytical conditions applied, and their chromatographic profiles were then compared to one of the porphyrin standard mixtures. Based on the characteristics of absorption spectra and retention time, it was found that the pink pigments synthesized by these *G. arilaitensis* strains under the studied conditions were composed of eight metal-free porphyrins, including UPI, UPIII, 7PI, 6PI, 5PI, CPI, CPIII, and MPIX. Considering the HPLC chromatograms, the degree of each porphyrin production was different. Regardless of precise quantitative measurement, the type strains Re117 and Po102 exhibited an ability to produce a high amount of CPIII, whereas MPIX was obviously formed by the strains Po102 and Stp101, but distinctly high by the strain Stp101.

Appendix A

The characteristic of UV–vis spectra of porphyrins that has been well recognized is that it consists of two distinct regions. Theoretically, this is a result of the change in electronic transitions from the ground state (S0) to the two lowest singlet excited states S1 and S2. The S0 → S1 transition allows a rise to weak Q bands in the visible region, while the S0 → S2 transition performs a strong Soret band in the near-ultraviolet region [29]. Corresponding to different vibrational modes in which the second excited singlet state (S2) can decline to the first excited singlet state (S1) and afterward undergo intersystem crossing to the first excited triplet state, the Q band comprises multiple peaks [33]. A typical porphyrin contains a very strong absorption of around 400 nm in the light spectrum, and several weaker absorptions between 450 and 700 nm.
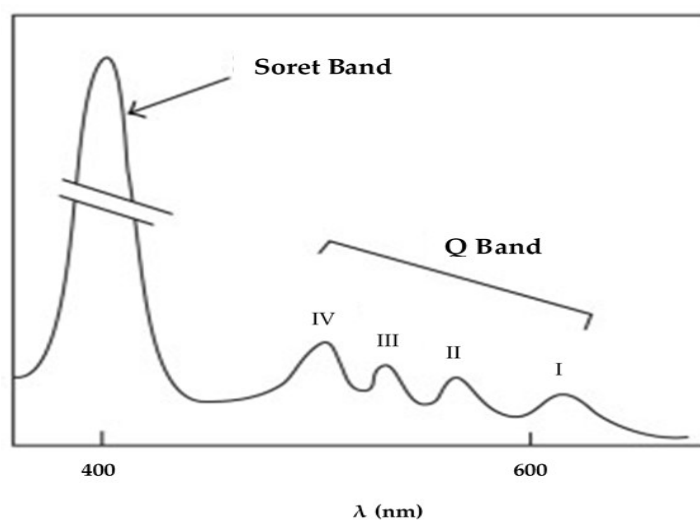

Figure A1. Typical absorption spectra of porphyrins [53].

References

1. Mounier, J.; Goerges, S.; Gelsomino, R.; Vancanneyt, M.; Vandemeulebroecke, K.; Hoste, B.; Brennen, N.M.; Scherer, S.; Swings, J.; Fitzgerald, G.F.; et al. Sources of the adventitious microflora of a smear-ripened cheese. *J. Appl. Microbiol.* **2006**, *101*, 668–681. [CrossRef] [PubMed]
2. Ritschard, J.S.; Amato, L.; Kumar, Y.; Müller, B.; Meile, L.; Schuppler, M. The role of the surface smear microbiome in the development of defective smear on surface-ripened red-smear cheese. *AIMS Microbiol.* **2018**, *4*, 622–641. [CrossRef]
3. Speight, K.C.; Schiano, A.N.; Harwood, W.S.; Drake, M.A. Consumer insights on prepackaged cheddar cheese shreds using focus groups, conjoint analysis, and qualitative multivariate analysis. *J. Dairy Sci.* **2019**, *102*, 6971–6986. [CrossRef] [PubMed]
4. Daly, D.F.M.; McSweeney, P.L.H.; Sheehan, J.J. Pink discoloration defect in commercial cheese: A review. *Dairy Sci. Technol.* **2012**, *92*, 439–453. [CrossRef]
5. Bottazzi, V.; Cappa, F.; Scolari, G.; Parisi, M.G. Occurring of pink discoloration in Grana cheese made with one-strain starter culture. *Sci. Tec. Latt. Casearia* **2000**, *51*, 67–74.
6. Marley, F.G.; Michel, V. Pinkish colouration in Cheddar cheese—Description and factors contributing to its formation. *J. Dairy Res.* **2001**, *68*, 327–332. [CrossRef] [PubMed]
7. Andersen, C.M.; Wold, J.P.; Mortensen, G. Light-induced changes in semi-hard cheese determined by fluorescence spectroscopy and chemometrics. *Int. Dairy J.* **2006**, *16*, 1483–1489. [CrossRef]

8. Guiliano, G.; Rosati, C.; Bramly, P.M. To dye or not to dye: Biochemistry of annatto unveiled. *Trends Biotechnol.* **2003**, *21*, 513–516. [CrossRef]

9. Sharma, P.; Segat, A.; Kelly, A.; Sheehan, J.J. Colorants in cheese manufacture: Production, chemistry, interaction, and regulation. *Compr. Rev. Food Sci. Food Saf.* **2020**, *19*, 1220–1242. [CrossRef] [PubMed]

10. Quigley, L.; O'Sullivan, D.J.; Daly, D.; O'Sullivan, O.; Burdikova, Z.; Vana, R.; Beresford, T.P.; Ross, R.P.; Fitzgerald, G.F.; McSweeney, P.L.H.; et al. *Thermus* and the pink discoloration defect in cheese. *Appl. Environ. Sci.* **2016**, *1*, e00023-16. [CrossRef]

11. Bockelmann, W. Smear-ripened cheeses. In *Encyclopedia of Dairy Sciences*, 2nd ed.; Fox, P.F., McSweeney, P.L.H., Eds.; Elsevier Inc.: Amsterdam, The Netherlands, 2011; pp. 753–766.

12. Flegler, A.; Runzheimer, K.; Kombeitz, V.; Mänz, A.T.; von Heilborn, D.H.; Etzbach, L.; Schieber, A.; Hőlzl, G.; Hüttler, B.; Woehle, C.; et al. *Arthrobacter bussei* sp. nov., a pink-colored organism isolated from cheese made of cow's milk. *Int. J. Syst. Evol. Microbiol.* **2020**, *70*, 3027–3036. [CrossRef]

13. Arai, A.; Igoshi, A.; Inoue, A.; Noda, K.; Tsutsuura, S.; Murata, M. Relationship between lactose utilization of lactic acid bacteria and browning of cheese during storage. *Biosci. Biotechnol. Biochem.* **2020**, *84*, 1886–1893. [CrossRef]

14. Jonnala, B.R.Y. Pink Discoloration in Cheese. Ph.D. Thesis, University College, London, UK, 14 January 2020. Available online: http://hdl.handle.net/10468/9501 (accessed on 22 July 2021).

15. Larpin-Laborde, S.; Imran, M.; Bonaïti, C.; Bora, N.; Gelsomino, R.; Goerges, S.; Irlinger, F.; Goodfellow, M.; Ward, A.C.; Vancanneyt, M.; et al. Surface microbial consortia from Livarot, a French smear-ripened cheese. *Can. J. Microbiol.* **2011**, *57*, 651–660. [CrossRef]

16. Irlinger, F.; Bimet, G.; Delettre, J.; Lefèvre, M.; Grimont, P.A.D. *Arhtrobacter bergerei* sp. nov. and *Arthrobacter arilaitensis* sp. nov., novel corynform species isolated from the surface of cheeses. *Int. J. Syst. Evol. Microbiol.* **2005**, *55*, 457–462. [CrossRef] [PubMed]

17. Sutthiwong, S.; Dufossé, L. Production of carotenoids by *Arthrobacter arilaitensis* strains isolated from smear-ripened cheeses. *FEMS Microbiol. Lett.* **2014**, 174–181. [CrossRef] [PubMed]

18. Guiffrida, D.; Sutthiwong, N.; Dugo, P.; Donato, P.; Cacciola, F.; Girad-Valenciennes, E.; Le Mao, Y.; Monnet, C.; Fouillaud, M.; Caro, Y.; et al. Characterisation of the C50 carotenoids produced by strains of the cheese-ripening bacterium *Arthrobacter arilaitensis*. *Int. Dairy J.* **2016**, *55*, 10–16. [CrossRef]

19. Sutthiwong, N.; Fouillaud, M.; Dufossé, L. The influence of pH, NaCl and the deacidifying yeasts *Debaryomyces hansenii* and *Kluyveromyces marxianus* on the production of pigments by the cheese-ripening bacteria *Arthobacter arilaitensis*. *Foods* **2018**, *7*, 190. [CrossRef] [PubMed]

20. Cleary, J.L.; Kolachina, S.; Wolfe, B.E.; Sanchez, L.M. Coproporphyrins III produced by the bacterium *Glutamicibacter arilaitensis* binds zinc and is upregulated by fungi in cheese rinds. *Appl. Environ. Sci.* **2018**, *3*, e0036-18. [CrossRef]

21. Dong, M.W. The essence of modern HPLC: Advantages, limitations, fundamentals, and opportunities. *LCGC North Am.* **2013**, *31*, 472–479.

22. Núñez, O.; Lucci, P. Application of liquid chromatography in food analysis. *Foods* **2020**, *9*, 1277. [CrossRef]

23. Galaup, P.; Sutthiwong, N.; Leclercq-Perlat, M.-N.; Valla, A.; Caro, Y.; Fouillaud, M.; Guérard, F.; Dufossé, L. First isolation of *Brevibacterium* sp. pigments in the rind of an industrial red-smear-ripened soft cheese. *Int. J. Dairy Technol.* **2015**, *68*, 144–147. [CrossRef]

24. Kumura, H.; Ohtsuyama, T.; Taitoh, M.; Koyanagi, H.; Kobayashi, K.; Wakamatsu, J.-I.; Ishizuka, S. Application of red pigment producing edible fungi for development of a novel type of functional cheese. *J. Food Process Preserv.* **2018**, e13707. [CrossRef]

25. Larroude, M.; Onésime, D.; Rué, O.; Nicaud, J.-M.; Rossignol, T. A *Yarrowia lipolytica* engineered for pyomelanin production. *Microorganisms* **2021**, *9*, 838. [CrossRef]

26. Benton, C.M.; Lim, C.K. Liquid chromatography: Porphyrins. In *Encyclopedia of Analytical Science*, 3rd ed.; Worsfold, P.J., Poole, C.F., Townshend, A., Miró, M., Eds.; Elsevier Inc.: Amsterdam, The Netherlands, 2013; pp. 209–230.

27. Vogelsang, D.F.; Maleczka, R.E., Jr.; Lee, A. HPLC characterization of *cis* and *trans* mixtures of double-decker shaped silsesquioxanes. *Silicon* **2018**, *11*, 5–13. [CrossRef]

28. Irlinger, F.; Layec, S.; Hélinck, S.; Dugat-Bony, E. Cheese rind microbial communities: Diversity, composition and origin. *FEMS Microbiol. Lett.* **2015**, *362*, 1–11. [CrossRef]

29. Giovannetti, R. The use of spectrophotometry UV-Vis for the study of porphyrins. In *Macro to Nano Spectroscopy*, 1st ed.; Uddin, J., Ed.; IntechOpen Ltd.: London, UK, 2012. [CrossRef]

30. Valicsek, Z.; Horváth, O. Application of the electronic spectra of porphyrins for analytical purposes: The effects of metal ions and structural distortions. *Microchem. J.* **2013**, *107*, 47–62. [CrossRef]

31. Mamardashvili, G.M.; Lazovskiy, D.A.; Khodov, I.A.; Efimov, A.E.; Mamardashvil, N.Z. New polyporphyrin arrays with controlled fluorescence obtained by diaxial Sn(IV)-porphyrin phenolates chelation with Cu2+ cation. *Polymers* **2021**, *13*, 829. [CrossRef] [PubMed]

32. Mason, M.G.; Ball, A.S.; Reeder, B.J.; Silkstone, G.; Nicholls, P.; Wilson, M.T. Extracellular heme peroxidases in *Actinomycetes*: A case of mistaken identity. *Appl. Environ. Microbiol.* **2001**, *67*, 4512–4519. [CrossRef]

33. Rostami, M.; Rafiee, L.; Hassanzadeh, F.; Dadrass, A.R.; Ghadam, A.K. Synthesis of some new porphyrins and their metalloderivatives as potential sensitizers in photo-dynamic therapy. *Res. Pharm. Sci.* **2015**, *10*, 504–513.

34. Sutthiwong, N.; Fouillaud, M.; Valla, A.; Caro, Y.; Dufossé, L. Bacteria belonging to the extremely versatile genus *Arthrobacter* as novel source of natural pigments with extended hue range. *Food Res. Int.* **2014**, *65*, 156–162. [CrossRef]

35. Lesage, S.; Xu, H.; Durham, L. The occurrence and roles of porphyrins in the environment: Possible implications for bioremediation. *Hydrol. Sci. J.* **1993**, *38*, 343–354. [CrossRef]

36. Kojima, I.; Maruhashi, K.; Fujiwara, Y.; Saito, T.; Kajiwara, M.; Mizutani, M. Identification of porphyrins produced from isopropanol by *Arthrobacter hyalinus*. *J. Ferment. Bioeng.* **1993**, *75*, 353–358. [CrossRef]

37. Scharf, R.; Mamet, R.; Zimmels, Y.; Kimchie, S.; Schoenfeld, N. Evidence for the interference of aluminum with bacterial porphyrin biosynthesis. *Biometals* **1994**, *7*, 135–141. [CrossRef] [PubMed]

38. Kajiwara, M.; Tokiwa, S.; Takatori, K.; Kojima, I. Properties of zinc uroporphyrin III produced from isopropanol by *Arthrobacter hyalinus*. *J. Ferment. Bioeng.* **1995**, *79*, 174–176. [CrossRef]

39. Yang, H.-S.; Hoober, J.K. Divergent pathways for δ-aminolevulinic acid synthesis in two species of *Arthrobacter*. *FEMS Microbiol. Lett.* **1995**, *134*, 259–263. [CrossRef]

40. Chaves, J.C.A.; Gregorutti dos Santos, C.; Aparecida de Miranda, E.G.; Arantes Junior, J.T.; Nantes, I.L. Free-base and metal complexes of 5,10,15,20-tetrakis(NMethyl Pyridinium L)porphyrin: Catalytic and therapeutic properties. In *Phthalocyanines and Some Current Applications*; Yilmaz, Y., Ed.; IntechOpen Ltd.: London, UK, 2017. [CrossRef]

41. Pérez-Urria, E.; Avalos, A. Approach to a comparative study of the metabolism of porphyrins and chlorophylls. *J. Nat. Sci.* **2015**, *3*, 1–16. [CrossRef]

42. Schobert, M.; Jahn, D. Regulation of heme biosynthesis in non-phototrophic bacteria. *J. Mol. Microbiol. Biotechnol.* **2002**, *4*, 287–294. [PubMed]

43. Zhang, J.; Kang, Z.; Chen, J.; Du, G. Optimization of the heme biosynthesis pathway for the production of 5-aminolevulinic acid in *Escherichia coli*. *Sci. Rep.* **2015**, *5*, 8584. [CrossRef]

44. Wolfe, B.E.; Button, J.E.; Santarelli, M.; Dutton, R.J. Cheese rind communities provide tractable systems for in situ and in vitro studies of microbial diversity. *Cells* **2014**, *158*, 422–433. [CrossRef] [PubMed]

45. Kastman, E.K.; Kamelamela, N.; Norville, J.W.; Cosetta, C.M.; Dutton, R.J.; Wolfe, B.E. Biotic interactions shape the ecological distributions of staphylococcus species. *mBio* **2016**, *7*, e01157-16. [CrossRef] [PubMed]

46. Frankenberg, N.; Moser, J.; Jahn, D. Bacterial heme biosynthesis and its biotechnological application. *Appl. Microbiol. Biotechnol.* **2003**, *63*, 115–127. [CrossRef]

47. Middleton, K.S.; Gunner, H.B. Porphyrin production by *Arthrobacter globiformis*. *Can. J. Microbiol.* **1968**, *14*, 1095–1103. [CrossRef]

48. Kortsee, G.J.J. Porphyrin Formation and Its Regulation in *Arthrobacter*. Ph.D. Thesis, Agricultural University, Wageningen, The Netherlands, 1969.

49. Bonkovsky, H.L.; Guo, J.-T.; Hou, W.; Li, T.; Narang, T.; Thapar, M. Porphyrin and Heme Metabolism and the Porphyrias. *Compr. Physiol.* **2013**, *3*, 365–401. [CrossRef] [PubMed]

50. Kwon, S.J.; de Boer, A.L.; Petri, R.; Schmidt-Dannert, C. High-level production of porphyrins in metabolically engineered *Escherichia coli*: Systematic extension of a pathway assembled from overexpressed genes involved in heme biosynthesis. *Appl. Environ. Microbiol.* **2003**, *69*, 4875–4883. [CrossRef] [PubMed]

51. Brazier, J.S. Analysis of the porphyrin content of fluorescent pus by absorption spectrophotometry and high performance liquid chromatography. *J. Med. Microbiol.* **1990**, *33*, 29–34. [CrossRef]

52. Yamane, Y.; Ooshima, H.; Kato, J. Overproduction of riboflavin by an *Arthrobacter* sp. mutant resistant to 5-fluorouracil. *Enzyme Microb. Technol.* **1993**, *15*, 877–880. [CrossRef]

53. Josefsen, L.B.; Boyle, R.W. Photodynamic therapy and the development of metal-based photosensitisers. *Met. Based Drugs* **2008**. [CrossRef] [PubMed]